when the molecular halogen (Lewis acid) was lighter than the halogen of the *tert*-butyl halide, exchange occurred. The bond dissociation energies in Table II show that all of the molecular halogens and interhalogens have comparable bond dissociation energies (within 10–15 Kcal/mol), while the C–X bond strength of the *tert*-butyl halide varies much more dramatically with the halogen. Consequently, the energetics of the exchange reaction between the *tert*-butyl halides and the molecular halogens is driven by the *tert*-butyl halide. On the other hand, the bond dissociation energy of the hydrogen halides varies greatly with the halogen and dominates the energetics of the exchange reaction between the hydrogen halides and the *tert*-butyl halides, favoring the light hydrogen halides.

To rationalize their kinetic data, Goldstein, Haines, and Hemmings[4] have invoked complex formation in solution as an initial step in the exchange reaction between the *tert*-butyl halides and the boron trihalides. The present study has permitted observation of several of these intermediate complexes as well as the products of the exchange reaction when the reaction conditions were varied. Overall, the experiments here support the concept that the molecular complex plays a role as an initial intermediate in the halogen-exchange reaction, although these reactions appear very rapid at room temperature and below.

Acknowledgment. We gratefully acknowledge support of this research by the National Science Foundation through Grant CHE 87-21969.

Registry No. *t*-BuCl, 507-20-0; *t*-BuBr, 507-19-7; ClF, 7790-89-8; Cl_2, 7782-50-5; Br_2, 7726-95-6; *t*-BuF, 353-61-7; $ClCH_2C(Cl)(CH_3)_2$, 594-37-6.

Ammonia Activation by Co^+, Ni^+, and Cu^+. M^+–NH_2 Bond Energies and M^+···NH_3 Adduct Lifetimes

D. E. Clemmer and P. B. Armentrout*,†

Department of Chemistry, University of Utah, Salt Lake City, Utah 84112 *(Received: September 10, 1990)*

Reactions of Co^+, Ni^+, and Cu^+ with ammonia are studied as a function of translational energy in a guided ion beam tandem mass spectrometer. All three metal ions form MH^+ and MNH_2^+ in endothermic reactions, but in contrast to reactions of Sc^+, Ti^+, and V^+ with ammonia, no MNH^+ formation is observed. Thresholds for the cross sections are interpreted to give the 298 K bond energies of $D°(Co^+–NH_2) = 2.66 \pm 0.09$ eV, $D°(Ni^+–NH_2) = 2.41 \pm 0.08$ eV, and $D°(Cu^+–NH_2) = 2.09 \pm 0.13$ eV. Details of the bonding interaction between M^+ and NH_2 are discussed. At low kinetic energies, formation of MNH_3^+ is also observed and found to be a result of secondary stabilizing collisions. Lifetimes for these adducts are determined and compared to values calculated by RRKM theory. Dual features in the cross section for adduct formation in the reaction of Co^+ with NH_3 (and ND_3) are shown to have drastically different lifetimes and are attributed to different structural isomers, Co^+···NH_3 and H–Co^+–NH_2.

Introduction

Recently, several laboratories have reported results concerning single ligand metal amide species for late transition metals. Ions such as $FeNH_2^+$, $CoNH_2^+$, and $RuNH_2^+$ have been observed in the gas phase[1,2] and neutral $NiNH_2$ and $CuNH_2$ have been studied in cryogenic argon matrices.[3] Primary amide complexes of these late transition metals are seldom formed in solution,[4] a result that has been attributed to the relatively weak bonds of these species.[4,5] Radecki and Allison reached this conclusion based on their observation that gas-phase Co^+ does not activate the C–N bond of amines.[5] They speculated that this was a result of a weak Co^+–NH_2 bond energy, <0.8 eV. In contrast, Buckner and Freiser used Fourier transform ion cyclotron resonance (FTICR) mass spectrometry to bracket the bond energy of Co^+–NH_2.[2] They reported a value of 2.82 ± 0.35 eV. No work on the thermochemistry of $NiNH_2^+$ or $CuNH_2^+$ has been reported.

In related work, Marinelli and Squires have examined the bonding interaction between transition-metal cations and ammonia.[6] In this experiment, $M^+(NH_3)_n$ (n = 1–4) for most of the first-row transition metals were formed in termolecular association reactions of atomic metal ions with ammonia in a flowing afterglow. By measuring the kinetic energy threshold for collision-induced dissociation (CID) of M^+–NH_3, these authors concluded that $D°(M^+–NH_3) = 2.55$ and 2.22 ± 0.2 eV for M = Co and Ni, respectively.

In the present study, we examine the kinetic energy dependence of the reactions of Co^+, Ni^+, and Cu^+ with ammonia by using guided ion beam mass spectrometry. This technique allows us to determine $D°(M^+–NH_2)$ for M = Co, Ni, and Cu, by directly measuring the energetic thresholds for the endothermic formation of MNH_2^+ from reaction of M^+ with NH_3. This study extends our previous work on the reactions of ammonia with Sc^+, Ti^+,[7] and V^+.[8] In this work, it was found that bond energies for MNH^+ and MNH_2^+ are stronger than for the isoelectronic carbon analogues, MCH_2^+ and MCH_3^+, respectively. (These ligands are isoelectronic in the sense that the heavy atom, N or C, has the same number of valence electrons with the same orbital hybridization.[9]) This enhancement was attributed to donation of the nitrogen lone pair electrons into *empty* 3d orbitals on the Sc^+, Ti^+, and V^+ metal ions. In the present work, we have the opportunity to examine whether this interaction changes when the metal 3d orbitals are singly occupied as for the late transition metals. This should further develop our understanding of the

† Camille and Henry Dreyfus Teacher-Scholar, 1987–1992.

(1) Buckner, S. W.; Freiser, B. S. *Polyhedron* **1989**, *7*, 1401–1406.
(2) Buckner, S. W.; Freiser, B. S. *J. Am. Chem. Soc.* **1987**, *109*, 4715–4716.
(3) Ball, D. W.; Hauge, R. H.; Margrave, J. L. *Inorg. Chem.* **1989**, *28*, 1599–1601.
(4) Discussions of transition metal amide chemistry in solution can be found in: Lappert, M. F.; Power, P. P.; Sanger, A. R.; Srivastava, R. C. *Metal and Metalloid Amides*; Ellis Horwood Limited: West Sussex, England, 1980.
(5) Radecki, B. D.; Allison, J. *J. Am. Chem. Soc.* **1984**, *106*, 946–952.
(6) Marinelli, P. J.; Squires, R. R. *J. Am. Chem. Soc.* **1989**, *111*, 4101–4103.
(7) Clemmer, D. E.; Sunderlin, L. S.; Armentrout, P. B. *J. Phys. Chem.* **1990**, *94*, 3008–3015.
(8) Clemmer, D. E.; Sunderlin, L. S.; Armentrout, P. B. *J. Phys. Chem.* **1990**, *94*, 208–217.
(9) Bent, H. A. *J. Chem. Educ.* **1966**, *43*, 170–186.

0022-3654/91/2095-3084$02.50/0

interactions of metals with lone pair electron donors.

We have recently communicated evidence for a long-lived oxidative addition reaction intermediate, $H-Co^+-NH_2$, formed in the reaction of Co^+ with ammonia.[10] Similar insertion species have been shown to exist in argon matrices at cryogenic temperatures[3] but had *not* been observed previously in gas-phase systems involving atomic metal ions. Measuring the thermochemistry associated with this insertion process gives insight into the potential energy surfaces for these transition metal ion–ammonia interactions. Further, the longevity of the proposed $H-Co^+-NH_2$ intermediate has stimulated us to measure the lifetimes of $M^+\cdots NH_3$ adducts as a function of reagent collision energy. These results are compared to lifetimes calculated by using RRKM theory. The kinetics of adduct decomposition provides additional insight into the chemical interactions between metal ions and lone pair electron donors. This information also aids in understanding the formation of metal–ammonia cluster ions in a high-pressure environment.

Experimental Section

General. Complete descriptions of the apparatus and experimental procedures are given elsewhere.[11] Metal ion production is described below. The ions are extracted from the source, accelerated, and focused into a magnetic sector momentum analyzer for mass analysis. Mass-selected ions are slowed to a desired kinetic energy and focused into an octopole ion guide which radially traps the ions. The octopole passes through a static gas cell containing the neutral reactant. Ammonia[12] pressures in the cell are kept low (between ~0.05 and 0.30 mTorr) so that multiple ion–molecule collisions are improbable. Product and unreacted beam ions are contained in the guide until they drift out of the gas cell where they are focused into a quadrupole mass filter to absolute cross sectioins as described previously.[11] Uncertainties in cross sections are estimated to be ±20%.

Laboratory ion energies relate to center-of-mass (CM) frame energies by $E_{CM} = E_{lab}m/(M + m)$, where M and m are the ion and neutral reactant masses, respectively. Below ~0.3 eV lab, energies are corrected for truncation of the ion beam energy distribution as described previously.[11] Absolute energy scale uncertainties are ±0.05 eV lab. Two effects broaden the data: the ion energy spread, which is independent of energy and has a fwhm of ~0.7 eV lab, and thermal motion of the neutral gas, which has a width of $\sim 0.47E_{CM}^{1/2}$ for these reactions.[13]

Ion Sources. The metal ions are produced by surface ionization (SI). In the SI source, $CoCl_2$, $NiCl_2$, or $CuBr_2$ is vaporized in an oven, and the vapor is directed toward a resistively heated rhenium filament. There, it decomposes and the resulting metal atoms are ionized. It is assumed that ions produced by SI equilibrate at the filament temperature and the state populations are governed by a Maxwell–Boltzmann distribution. The validity of this assumption has been discussed previously.[14] The temperature of the SI filament used in these experiments is 2250 ± 100 K. Under these conditions the beams comprise mostly ground-state ions, 84% $Co^+(^3F)$ with 16% $Co^+(^5F)$ first excited state also present, 99% $Ni^+(^2D)$, and 100% $Cu^+(^1S)$. Exact populations and energies of the low-lying states populated in these SI beams have been tabulated previously.[15]

Thermochemical Analyses. Theory[16,17] and experiment[18,19] indicate that cross sections for endothermic reactions can be analyzed by using eq 1, which involves an explicit sum of the

$$\sigma(E) = \sum_i g_i\sigma_0(E - E_0 + E_i)^n/E \qquad (1)$$

contributions of individual electronic states and spin–orbit levels, denoted by i, weighted by their populations, g_i. Here, σ_0 is a scaling factor that is assumed to be the same for all states, E is the relative kinetic energy, n is an adjustable parameter, E_0 is the threshold for reaction of the lowest electronic level of the ion [$J = 4$ for Co^+, $J = 5/2$ for Ni^+, and $J = 0$ for Cu^+] and E_i is the electronic excitation of each particular J level. The σ_0, n, and E_0 parameters are obtained by using a nonlinear least-squares analysis to give the best fit to the data after convoluting over the neutral and ion kinetic energy distributions as described previously.[11] Error limits for E_0 are calculated from the range of values for different data sets and the absolute error in the CM energy scale, ±0.03 eV. In all cases, the energy broadening is sufficiently large that cross-section features attributable to individual electronic levels (including the ^5F state of Co^+) cannot be observed.

A modified form of eq 1 accounts for depletion of the product ion at higher energies. This model, described in detail previously,[20] depends on E_D, the energy where a dissociation channel or a competing reaction can begin. The use of this model is required for analysis of the metal amide ion cross sections since the shape of these cross sections is heavily influenced by competition with formation of the metal hydride ion, as discussed below. Similar observations have been made previously for other Cu^+ and Ni^+ reaction systems.[15] Analysis of the cross sections without accounting for this competition can lead to spuriously low thresholds. In addition, the use of this modified form allows the data to be analyzed over a much broader energy region, thereby defining the optimum parameters of eq 1 more accurately.

To calculate metal–ligand bond energies, we assume that E_0 is the enthalpy difference between reactants and products. This implies that there are no activation barriers in excess of the endothermicity, an assumption which is often true for ion–molecule reactions.[21] We also assume that the ammonia reactant and the

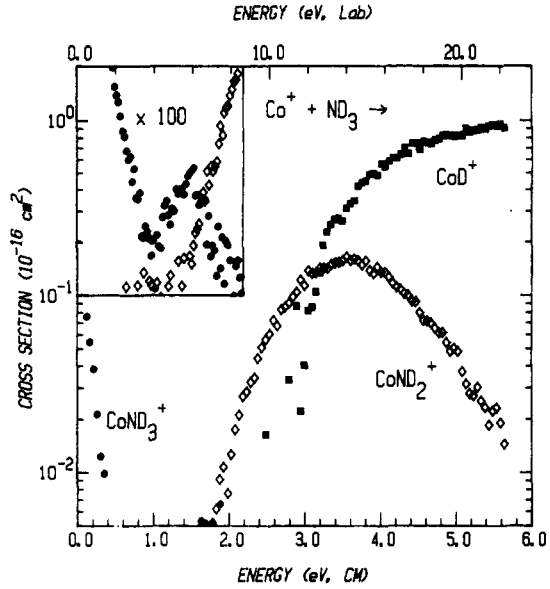

Figure 1. Variation of product cross sections for reaction of deuterated ammonia with Co^+ produced by SI as a function of translational energy in the center-of-mass frame (lower scale) and the laboratory frame (upper scale). Results are shown for CoD^+ (closed squares), $CoND_2^+$ (open diamonds), and $CoND_3^+$ (closed circles). The inset shows more detailed results at low energies for $CoND_2^+$ and $CoND_3^+$ cross sections expanded by a factor of 100. Results are shown for an ND_3 pressure of ~0.2 mTorr.

(10) Clemmer, D. E.; Armentrout, P. B. *J. Am. Chem. Soc.* **1989**, *111*, 8280–8281.
(11) Ervin, K. M.; Armentrout, P. B. *J. Chem. Phys.* **1985**, *83*, 166–189.
(12) Before usage, NH_3 (Matheson, 99.99%) and $^{14}ND_3$ (Cambridge Isotope Laboratories 99.5%) were subjected to multiple freeze–pump–thaw cycles with liquid nitrogen to remove volatile impurities.
(13) Chantry, P. J. *J. Chem. Phys.* **1971**, *55*, 2746.
(14) Sunderlin, L. S.; Armentrout, P. B. *J. Phys. Chem.* **1988**, *92*, 1209–1219.
(15) Elkind, J. L.; Armentrout, P. B. *J. Phys. Chem.* **1986**, *90*, 6576–6586.
(16) See discussion in: Aristov, N.; Armentrout, P. B. *J. Am. Chem. Soc.* **1986**, *108*, 1806–1819.
(17) Chesnavich, W. J.; Bowers, M. T. *J. Phys. Chem.* **1979**, *83*, 900–905.
(18) Armentrout, P. B.; Beauchamp, J. L. *J. Chem. Phys.* **1981**, *74*, 2819–2826. Armentrout, P. B.; Beauchamp, J. L. *J. Am. Chem. Soc.* **1981**, *103*, 784–791.
(19) Sunderlin, L.; Aristov, N.; Armentrout, P. B. *J. Am. Chem. Soc.* **1987**, *109*, 78–89.
(20) Weber, M. E.; Elkind, J. L.; Armentrout, P. B. *J. Chem. Phys.* **1986**, *84*, 1521–1529.

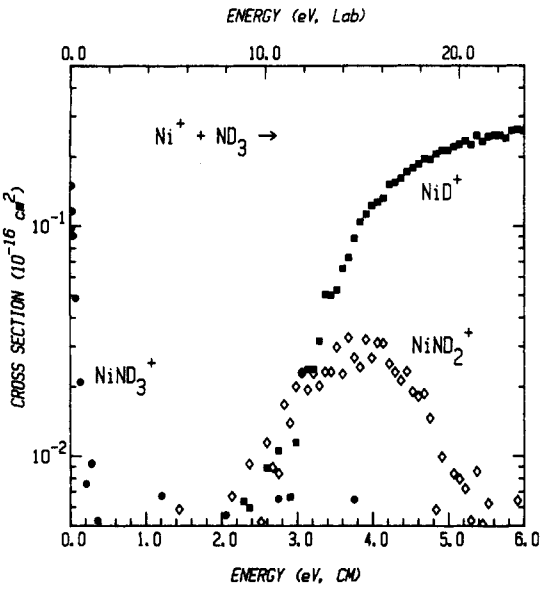

Figure 2. Variation of product cross sections for reaction of deuterated ammonia with Ni^+ produced by SI as a function of translational energy in the center-of-mass frame (lower scale) and the laboratory frame (upper scale). Results are shown for NiD^+ (closed squares), $NiND_2^+$ (open diamonds), and $NiND_3^+$ (closed circles). Results are shown for an ND_3 pressure of 0.14 mTorr.

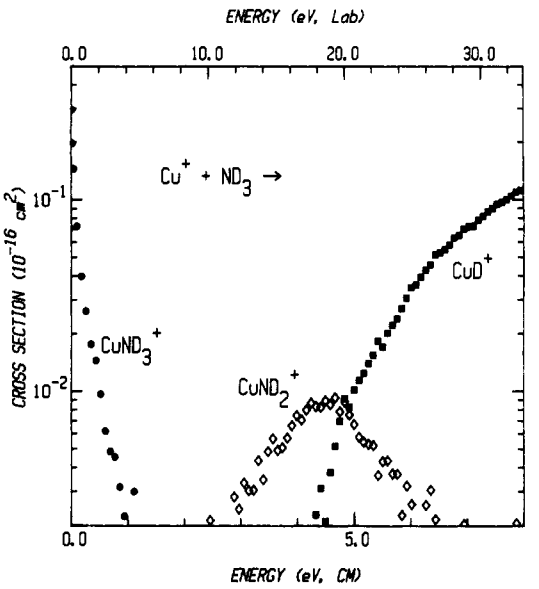

Figure 3. Variation of product cross sections for reaction of deuterated ammonia with Cu^+ produced by SI as a function of translational energy in the center-of-mass frame (lower scale) and the laboratory frame (upper scale). Results are shown for CuD^+ (closed squares), $CuND_2^+$ (open diamonds), and $CuND_3^+$ (closed circles). Results are shown for an ND_3 pressure of 0.2 mTorr.

products formed at the threshold of an endothermic reaction are characterized by a temperature of 298 K in all degrees of freedom. Thus, we make no correction for the energy available in internal modes of the neutral reactant.

Results

Figures 1, 2, and 3 show cross sections for reactions of ND_3 with Co^+, Ni^+, and Cu^+, respectively, when the metal ions are produced by SI at 2250 ± 100 K. Cross sections for the reaction of Co^+ with NH_3 have been published previously[10] and are qualitatively similar to Figure 1 for all data channels. Three products are formed in all three systems, reactions 2–4. In

$$M^+ + ND_3 \rightarrow MD^+ + ND_2 \quad (2)$$
$$\rightarrow MND_2^+ + D \quad (3)$$
$$\rightarrow MND_3^+ \quad (4)$$

contrast to the reactions of Sc^+, Ti^+,[7] and V^+,[8] no other products (such as MND^+ and MN^+) are observed, although a careful search for these products was conducted. The cross sections for formation of these products must be smaller than 0.005 Å^2. Results for reaction of M^+ with ND_3 are shown here to exclude possible contributions to the cross sections from reaction of M^+ with O_2, a minor contaminant. For NH_3, the MO^+ product ion has the same mass as the metal amide ion, MNH_2^+. Since $\sigma(MNH_2^+)$ is very small, Figures 1–3, O_2 concentrations as low as 1 part in 10^4 could affect the appearance of $\sigma(MNH_2^+)$.[22] For ND_3, MO^+ also has the same mass as MND^+, but this species is not observed as a product, as confirmed by experiments with NH_3 in all three systems. The use of ND_3 also improves mass resolution since product masses differ by at least $m(D) = 2$ amu. In the following, analyses of individual reaction channels rely mostly on ND_3 data; however, where available, data taken with NH_3 are also considered.

In all three systems, the dominant reaction at high energies is formation of MD^+, Figures 1–3. This product can conceivably dissociate beginning at 4.81 eV = $D°(ND_2–D)$,[23] the thermodynamic threshold for the overall reaction 5. $\sigma(MD^+)$ continues

$$M^+ + ND_3 \rightarrow M^+ + D + ND_2 \quad (5)$$

to rise above this energy, indicating that the excess energy must be contained in either translational energy or internal energy of the ND_2 neutral product. This behavior is typical of ionic metal hydride product cross sections arising from reactions of M^+ with polyatomic neutral molecules.[7,8,14,24]

Reaction 3 is clearly endothermic in all three systems, Figures 1–3, and dominates the reactivity over a brief energy range for each system. While the onsets and peaks of the cross sections for MND_2^+ formation vary for these metals, the general shape of the reaction cross sections are similar. The cross sections for $CoND_2^+$, $NiND_2^+$, and $CuND_2^+$ peak at ~3.6, ~3.8, and ~4.3 eV, respectively. The decline in these cross sections above these energies cannot be due to decomposition to form MND^+ or MN^+, since we do not observe these products. Nor can they be due to the dissociation process 5, since this requires 4.81 eV. Instead, the production of MND_2^+ must be suppressed by competition with MD^+ formation, reaction 2. In all cases, MD^+ has a cross section which rises rapidly near the peak in the MND_2^+ cross section. Similar competition between formation of MD^+ and MND_2^+ was observed for the reactions of Sc^+, Ti^+, and V^+ with ammonia.[7,8]

At the lowest kinetic energies, formation of adduct ions, reaction 4, is the only process observed for all three metals. This is in contrast to the reactions of Sc^+, Ti^+, and V^+ with ammonia, where no adduct was observed and instead MND^+ was formed at low energies. Adduct formation must be exothermic and barrierless since these cross sectioins increase with decreasing energy to as low an energy as we can measure. These cross sections are found to depend linearly upon the ammonia pressure for all three metals. This is illustrated in Figure 4 by $\sigma(CoNH_3^+)$ and $\sigma(CoND_3^+)$ measured at a kinetic energy of 0.05 eV.

(21) Boo, B. H.; Armentrout, P. B. *J. Am. Chem. Soc.* **1987**, *109*, 3549–3559. Ervin, K. M.; Armentrout, P. B. *J. Chem. Phys.* **1986**, *84*, 6738–6749. Ervin, K. M.; Armentrout, P. B. *J. Chem. Phys.* **1987**, *86*, 2659–2673. Elkind, J. L.; Armentrout, P. B. *J. Phys. Chem.* **1984**, *88*, 5454–5456.

(22) Cross sections for MO^+ formation from the $M^+ + O_2$ (M = Co, Ni, Cu) can be found in: Fisher, E. R.; Elkind, J. L.; Clemmer, D. E.; Georgiadis, R.; Loh, S. K.; Aristov, N.; Sunderlin, L. S.; Armentrout, P. B. *J. Chem. Phys.* **1990**, *93*, 2676–2691.

(23) The heats of formation used to calculate $D°_{298}(H_2N–H) = 4.69_5 \pm 0.01_4$ eV are $\Delta_f H_{298}(H) = 2.259 \pm 0.000$, $\Delta_f H_{298}(NH_3) = -0.476 \pm 0.004$ eV from: Chase, M. W.; Davies, C. A.; Downey, J. R.; Frurip, D. J.; McDonald, R. A.; Syverud, A. N. *J. Phys. Chem. Ref. Data* **1985**, *14*, (Suppl. No. 1) (JANAF Tables). $\Delta_f H_{298}(NH_2) = 1.96 \pm 0.009$ eV was derived from $\Delta_f H°_0$ results from: Anderson, W. R. *J. Phys. Chem.* **1989**, *93*, 530–536. The JANAF Tables can be used to calculate that $D°(ND_2–D) > D°(H_2N–H)$ by 0.118 eV, which means that $D°(D_2N–D) = 4.813$ eV.

(24) Aristov, N.; Amentrout, P. B. *J. Phys. Chem.* **1987**, *91*, 6178–6188.

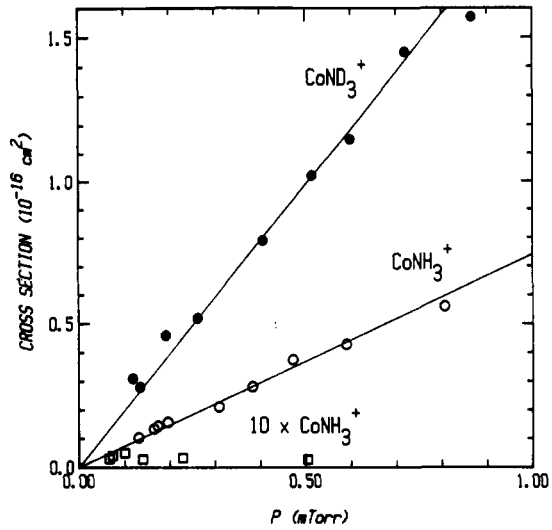

Figure 4. Variation of $\sigma(CoNH_3^+)$ and $\sigma(CoND_3^+)$ as a function of ammonia pressure in mTorr. Results are shown for collision energies in the center-of-mass frame at 0.05 eV (circles) and 1.5 eV for $CoNH_3^+$ (squares, ×10).

TABLE I: Summary of Parameters for Eq 1

product	E_0, eV	σ_0	n	E_D
CoH^+	2.84 (0.24)	2.7 (0.8)	0.8 (0.3)	
CoD^+	2.91 (0.22)	1.4 (0.7)	1.3 (0.3)	
$CoNH_2^+$	2.00 (0.10)	0.27 (0.08)	1.1 (0.1)	2.9 (0.1)
$CoND_2^+$	2.19 (0.10)	0.45 (0.03)	1.2 (0.1)	3.8 (0.2)
NiD^+	3.03 (0.21)	0.6 (0.2)	1.6 (0.5)	
$NiND_2^+$	2.40 (0.08)	0.13 (0.03)	1.2 (0.2)	3.8 (0.1)
CuD^+	3.83 (0.31)	0.04 (0.01)	2.3 (0.2)	
$CuND_2^+$	2.72 (0.13)	0.02 (0.01)	1.3 (0.2)	4.5 (0.1)

In addition to the exothermic features exhibited by $\sigma(CoNH_3^+)$ and $\sigma(CoND_3^+)$ at low energies, these cross sections also display a second feature beginning near 1.0 eV, Figure 1, that is not observed in the Ni and Cu systems. The key difference between this endothermic feature and the exothermic portions of $\sigma(CoNH_3^+)$ and $\sigma(CoND_3^+)$ is that the magnitude of the former is *not* dependent upon the ammonia pressure, Figure 4. This pressure independence indicates that the $CoNH_3^+$ ($CoND_3^+$) formed at these energies lives in excess of the ion flight time between the collision cell and the detector (~60 μs) without the need for a stabilizing collision or possibly that this species radiatively stabilizes on this time scale. A rough analysis[25] of these endothermic features gives an apparent onset of ~0.8 eV and peak at ~1.3 eV for $\sigma(CoNH_3^+)$,[10] and a threshold of ~0.9 eV and maximum at ~1.6 eV for $\sigma(CoND_3^+)$, Figure 1.

Threshold Analysis. Cross sections for reactions 2 and 3 were analyzed by using eq 1 with populations and energies of electronic states given previously,[15] and the parameters given in Table I. In the case of Co^+, results for reaction with NH_3 were also analyzed. Results for Ni^+ reactions with NH_3 are consistent with those for the ND_3 system but were sufficiently scattered that unambiguous analysis is not possible.

The 298 K bond energies for MD^+ and MH^+ have been measured previously (Table II).[15] These values, combined with the appropriate ammonia thermochemistry, lead to predicted reaction 2 thresholds of 2.74 ± 0.06, 3.04 ± 0.08, and 3.80 ± 0.13 eV for M = Co, Ni, and Cu, respectively, and a threshold for CoH^+ formation of 2.68 ± 0.06 eV. These calculated values are all within experimental error of the thresholds determined here, Table I. This demonstrates that there are no significant barriers above the reaction endothermicity.

For the metal amide ions, combining the measured thresholds listed in Table I with $D°(ND_2–D)$ = 4.81 eV[23] gives $D°(Co^+–ND_2)$ = 2.62 ± 0.10 eV, $D°(Ni^+–ND_2)$ = 2.41 ± 0.08 eV, and $D°(Cu^+–ND_2)$ = 2.09 ± 0.10 eV. For $CoNH_2^+$, the measured threshold is combined with $D°(NH_2–H) = 4.69_5 \pm 0.01_4$ eV[23] to yield $D°(Co^+–NH_2)$ = 2.69 ± 0.10 eV. Previously, we have found that $D°(M^+–NH_2) \approx D°(M^+–ND_2)$ for M = Sc, Ti, and V,[7,8] as a result that is clearly true for cobalt and presumably for nickel and copper as well. Thus, our final values are listed in Table II as $D°(M^+–NH_2)$. For M = Ni and Cu, this value is simply equal to $D°(M^+–ND_2)$, while for M = Co, it is the average of $D°(Co^+–ND_2)$ and $D°(Co^+–NH_2)$.

TABLE II: Bond Dissociation Energies (eV) at 298 K

M^+	$D°(M^+–H)$[a]	$D°(M^+–CH_3)$	$D°(M^+–NH_2)$	$D°(M^+–NH_3)$
Sc	2.48 (0.09)[b]	2.56 (0.13)[c]	3.69 (0.07)[d]	
Ti	2.35 (0.11)[e]	2.49 (0.12)[f]	3.69 (0.13)[d]	
V	2.09 (0.06)[g]	2.17 (0.10)[h]	3.18 (0.10)[i]	2.25 (0.2)[j]
Co	2.02 (0.06)[k]	2.13 (0.15)[l]	2.66 (0.09)[m]	2.55 (0.2)[j]
Ni	1.72 (0.08)[k]	1.95 (0.10)[l]	2.41 (0.08)[m]	2.22 (0.2)[j]
Cu	0.96 (0.13)[k]	1.28 (0.07)[l]	2.09 (0.13)[m]	2.14,[n] ~2.6[m]

[a] These 298 K values are changed from 0 K values by adding $3kT/2$. For deuterated systems, $D°(M^+–D)$ is greater than $D°(M^+–H)$ by 0.05 eV. [b] Elkind, J. L.; Sunderlin, L. S.; Armentrout, P. B. *J. Phys. Chem.* **1989**, *93*, 3151–3158. [c] Reference 19. [d] Reference 7. [e] Elkind, J. L.; Armentrout, P. B. *Int. J. Mass Spectrom. Ion Processes* **1988**, *83*, 259–284. [f] Sunderlin, L. S.; Armentrout, P. B. *Int. J. Mass Spectrom. Ion Processes* **1989**, *94*, 149–177. [g] Elkind, J. L.; Armentrout, P. B. *J. Phys. Chem.* **1985**, *89*, 5626–5636. [h] Reference 24. [i] Reference 8. [j] Reference 6. [k] Reference 15. [l] Georgiadis, R.; Fisher, E. R.; Armentrout, P. B. *J. Am. Chem. Soc.* **1989**, *111*, 4251–4262. [m] This study. [n] Reference 36.

Discussion

Thermochemistry. Our value for the $Co^+–NH_2$ bond energy is within the broad limits 2.47 eV ≤ $D°(Co^+–NH_2)$ ≤ 3.17 eV as bracketed by Buckner and Freiser using FTICR.[2] This refutes the weak bond energy for $Co^+–NH_2$ suggested by Radecki Allison[5] and verifies that the failure of Co^+ to activate the C–N bond of amines is not due to thermodynamic considerations. No literature thermochemistry is available for comparison to the $D°(Ni^+–NH_2)$ and $D°(Cu^+–NH_2)$ values measured here.

As discussed by Mavridis et al.[26] and in Appendix A, an amide ligand might interact in two ways with an atomic metal ion: one is dominated by a covalent bond and the other by a dative bond. For covalent bonding, we imagine that NH_2 will bond like its CH_3 isoelectronic counterpart,[27] by forming a covalent single bond primarily with the 4s orbital on M^+. However, the bonding interaction of M^+ with NH_2 does not parallel that with CH_3 exactly. As shown in Table II, the bond strengths for $M^+–NH_2$ are all stronger than those for MCH_3^+ for both the metals studied here and for M = Sc, Ti, and V. For the early transition metals, $D°(M^+–NH_2)$ is greater than $D°(M^+–CH_3)$ by ~1.1 eV, while for M = Cu, the increase is 0.8 eV, and for M = Co and Ni, it is ~0.5 eV. For the early transition metals, we have previously suggested that this enhancement in bond energy for $M^+–NH_2$ compared to $M^+–CH_3$ is due to a bonding interaction between the empty 3d orbitals on Sc^+, Ti^+, and V^+ and the lone pair electrons on nitrogen.[7,8] Since the late transition metals have no empty 3d orbitals, the lone pair enhancement of the metal–amide bond energies cannot be as great as for the early transition metals. Since an increase is observed for these late models, we speculate that there is a net bonding interaction due to donation of the nitrogen lone pair electrons into half-filled metal 3d orbitals (a bond order of 1/2).

A dative mode of bonding between NH_2 and M^+ is suggested by the fairly large bond strength measured for $CuNH_2^+$. Because Cu^+ has a very stable, closed-shell d^{10} electron configuration, it is energetically costly to put this ion into the $4s^13d^9$ configuration necessary to form a covalent bond.[27,28] Instead, $Cu^+(3d^{10})$ could

(25) The deconvolution was accomplished by fitting the exothermic portion of $\sigma(CoNH_3^+)$ with a power law and subtracting the fit from the original cross section. This leaves only the endothermic feature of the cross section.

(26) Mavridis, A.; Kunze, K. L.; Harrison, J. F.; Allison, J. *ACS Symp. Ser.* **1990**, *428*, 263–278.
(27) Armentrout, P. B. *ACS Symp. Ser.* **1990**, *428*, 18–33.
(28) Elkind, J. L.; Armentrout, P. B. *Inorg. Chem.* **1986**, *25*, 1078–1080.

TABLE III: Rate Constants for Stabilization of $M^+\cdots NH_3$ and $M^+\cdots ND_3$ Adducts

species	$k_s\sigma/k_d$, 10^{-30} cm^5	k_s,[a] 10^{-9} cm^3/s	k_d,[b] 10^7 s^{-1}	τ(exp),[c] ns	τ(RRKM), ns
$CoNH_3^+$	2.3 (0.2)	3.2	5.4 (0.4)	19 (2)	4.0
$CoND_3^+$	6.1 (0.8)	3.0	1.9 (0.3)	53 (7)	24.4
$NiNH_3^+$	0.2 (0.4)	3.2	67 (46)	1.5 (3)	2.0
$NiND_3^+$	0.9 (0.3)	3.0	13 (7)	8 (3)	10.5
$CuNH_3^+$	2.9 (0.4)	3.2	4.3 (0.6)	23 (3)	1.6
$CuND_3^+$	3.2 (2.1)	3.0	3.6 (2.4)	28 (19)	8.7

[a] These values are upper limits calculated by using the strong collision assumption. [b] These values are upper limits calculated as described in the text. [c] These values are lower limits calculated as described in the text.

form a dative bond with NH_2 by accepting the lone pair of electrons to the nitrogen into its empty 4s orbital. This suggests that $D°(M^+–NH_2)$ should be comparable to $D°(M^+–NH_3)$. Indeed, the data of Table II show that this is approximately true for M = Co, Ni, and Cu, but for V, $D°(V^+–NH_2)$ is much stronger than $D°(V^+–NH_3)$. This difference must be due to an additional covalent bond between one of the unpaired metal 3d electrons and the unpaired electron on NH_2; see Appendix A. This interaction has been demonstrated by calculations of Mavridis et al.[26] for the particular case of $ScNH_2^+$ and it seems likely that this effect will occur for all the early transition metal amide ions.

It should be noted that, for the early transition metals, the two modes of bonding lead to molecular orbital (MO) configurations for MNH_2^+ that are probably indistinguishable. For the late transition metals, the two bonding modes may lead to different spin states for the MNH_2^+ molecules, as described in detail in Appendix A. Theoretical calculations will be very helpful in clarifying the interactions between atomic metal ions and NH_2 and in deciding which of these two bonding modes is most favorable for the late transition metal amide ions. Such calculations can also consider other contributions to the bonding, such as electrostatic interactions,[29] that are not easily considered in the very qualitative discussion above.

Lifetime of Adduct Intermediates. The lifetimes of reaction intermediates are measured by a method which parallels[30] one introduced by Tolbert and Beauchamp.[31] The formation of metal ion–ammonia adducts presumably occurs via the mechanism shown in Scheme I. Here, $[M^+\cdots NH_3]^*$ is formed with a bi-

SCHEME I

$$M^+ + NH_3 \underset{k_d}{\overset{k_c}{\rightleftharpoons}} [M^+\cdots NH_3]^* \xrightarrow{k_s(NH_3)} MNH_3^+$$

molecular rate constant of k_c (the total collision rate constant) and may be either stabilized by further collisions with ammonia (with a bimolecular rate constant of k_s) or dissociate back to reactants (with a unimolecular rate constant of k_d). From this mechanism, the pressure-dependent cross section for adduct formation can be expressed by eq 6, where σ_c is the total collision

$$\sigma_a(P) = k_s\sigma_c(P\beta)/(k_d + k_sP\beta) \quad (6)$$

cross section ($\sigma_c = vk_c$, where v is the relative velocity of the colliding species), $\beta = 1/k_BT$, k_B is the Boltzmann constant, and P and T are the neutral gas pressure and temperature, respectively. In the present experiments, the pressures used are sufficiently low that eq 6 simplifies to eq 7. This is verified by the linearity of

$$\sigma_a(P) = k_s\sigma_cP\beta/k_d \quad (7)$$

the data as plotted in Figure 4. Thus, the slopes of these data are $k_s\sigma_c\beta/k_d$. Slopes determined by a linear regression analysis of all systems are listed in Table III after dividing by β, 3.11×10^{-17} cm^3 Torr. In all cases, linear least-squares fits to the data have intercepts that are zero within our experimental error, indicating that there are no obvious radiative contributions to the lifetimes of these species.

In order to progress further, we make two assumptions: (1) the strong collision assumption that only one collision is necessary for stabilization of the adduct, and (2) the cross section for formation of the adduct, σ_c, occurs at the collision limit. Upper limits for k_s and σ_c can be calculated by using the locked dipole (LD) rate model, eq 8.[32] In eq 8, α is the polarizability of ammonia

$$\sigma_{LD}(E) = 2\pi e[(\alpha/2E)^{1/2} + \mu/2E] \quad (8a)$$

$$k_{LD}(E) = v\sigma_{LD}(E) \quad (8b)$$

(2.16 Å^3),[33] μ is the dipole moment of ammonia (1.46 D),[33] and e is the electron charge. For all systems, the locked dipole cross section at 0.05 eV is the same, σ_c = 386 Å^2. Values for k_s calculated for stabilization by collision with ammonia[34] are given in Table III. These values can be combined with the measured values of the slopes, $k_s\sigma_c/k_d$, to yield upper limits to k_d and lower limits to the lifetimes ($\tau = k_d^{-1}$) of the adduct intermediates. These are listed in Table III.

Two important results are apparent in Table III. First, the lifetimes for M^+ interacting with ND_3 are longer than for interaction with NH_3. This must be due to the lower vibrational frequencies and thus the higher density of states for MND_3^+ compared with MNH_3^+. Complementary evidence for this effect comes from our previous studies of the exothermic dehydrogenation reactions of Sc^+, Ti^+, and V^+ with NH_3 and ND_3 to produce MNH^+ and MND^+.[7,8] Reevaluation of the low-energy portions of the cross sections for these products indicates that, at ~0.05 eV, $\sigma(MND^+)/\sigma(MNH^+)$ is ~2.0 for all three metals. This enhancement presumably occurs because a longer metal ion–ammonia adduct lifetime allows the rearrangement required for the dehydrogenation process to compete more efficiently with back dissociation to re-form reactants.

The second result apparent from Table III is that the lifetimes for the $CoNH_3^+$ and $CuNH_3^+$ adducts are comparable, while the lifetime of the $NiNH_3^+$ adduct is more than an order of magnitude smaller. This is consistent with the relative binding energies of the cobalt and nickel ion–ammonia complexes measured by Marinelli and Squires.[6] Further, the comparison of the cobalt and copper results suggests that $D°(Cu^+–NH_3)$ should be similar to $D°(Co^+–NH_3)$. This result also shows that formation of the metal ion–ammonia complexes in a high-pressure environment should be much easier for Co and Cu than for Ni.

The observation of metal ion–ammonia adducts in this work can be contrasted with our failure to observe such species in the reactions of Sc^+, Ti^+, and V^+ with NH_3 and ND_3, even at ammonia pressures up to ~0.5 mTorr.[7,8] Presumably our inability to detect adduct formation for these three metals is due to shorter lifetimes for these adducts, a result which is at least partially due to the availability of the exothermic dehydrogenation reaction.

RRKM Calculations of Adduct Lifetimes. To examine whether the lifetimes of the metal ion–ammonia adducts determined experimentally are reasonable, we can compare these values with those calcualted by using RRKM theory.[35] The details of these

(29) While the polarizabilities of the CH_3 and NH_2 radicals are probably comparable, the dipole moment of NH_2 is presumably much greater.

(30) Differences between our experiment and that of Tolbert and Beauchamp are that we use no additional stabilization gas and there are no exothermic primary reactions in the present systems.

(31) Tolbert, M. A.; Beauchamp, J. L. *J. Am. Chem. Soc.* **1986**, *108*, 7509–7517.

(32) Moran, T. F.; Hamill, W. H. *J. Chem. Phys.* **1963**, *39*, 1413–1422.

(33) Rothe, E. W.; Bernstein, R. B. *J. Chem. Phys.* **1959**, *31*, 1619–1627.

(34) The energy of this second collision is the relative kinetic energy for a collision between the adduct and a stationary ammonia molecule, $E = E_{CM}M/(2m + M)$, plus the average kinetic energy of the ammonia molecule in this relative mass frame, $(3kT/2)(m + M)/(2m + M)$.

(35) Robinson, P. J.; Holbrook, K. A. *Unimolecular Reactions*; Wiley: New York, 1972.

calculations are included in Appendix B. These calculations use the experimental Co^+–NH_3 and Ni^+–NH_3 bond energies measured by Marinelli and Squires[6] and a theoretical value for $D°(Cu^+–NH_3)$.[36] Table III gives the calculated lifetimes for all metal adduct ions at the same energy conditions as the listed experimental results. These results are in reasonable agreement with the experimental values in all cases but $CuNH_3^+$. This agreement validates the strong collision assumption made above, since otherwise the experimental lifetimes would be larger and thus in worse agreement with the RRKM theory results. We also note that calculated values of τ for the deuterated systems are larger than values for the nondeuterated molecules, in agreement with our experimental results.

The only difference between the RRKM calculations for different metals is the M^+–ammonia bond energies. As noted above, comparison of the Co^+–NH_3 and Cu^+–NH_3 adduct lifetimes and cross sections suggests that these species should have similar bond energies, while the theoretically calculated value for $D°(Cu^+–NH_3)$ is much less than the experimentally measured value for $D°(Co^+–NH_3)$ (Table II). An alternate value for one of these bond energies can be derived by comparing our calculated and experimental adduct lifetimes. Rather than make a direct comparison between τ(exp) and τ(RRKM), we ensure that the relative values for the cobalt and copper adducts that are calculated agree with the relative values that are determined experimentally. Table III shows that the experimental ratio of $\tau(CuNH_3^+)/\tau(CoNH_3^+) \approx 1.2$. (We consider only $CuNH_3^+$ since better experimental data is available for this complex than for $CuND_3^+$.) To reproduce this ratio with the RRKM calculations, we require that $D°(Cu^+–NH_3) \approx 2.6$ eV given that $D°(Co^+–NH_3) = 2.55$ eV.

Reaction Mechanisms. In the reactions of Co^+, Ni^+, and Cu^+ with ammonia, all products observed are spin allowed from ground-state reactants, and therefore, there are no obvious electronic restrictions to these reactions. The reaction mechanism proposed here parallels the ideas used previously to describe the interactions of ammonia with Sc^+, Ti^+, and V^+.[7,8] An obvious first step in a mechanism that explains the observed competition between MH^+ and MNH_2^+ products is oxidative addition of the N–H bond at the metal center to form $H–M^+–NH_2$, intermediate I. At elevated energies, I decomposes via M–H or M–N bond cleavage to form $MNH_2^+ + H$ or $MH^+ + NH_2$, respectively. Formation of MNH_2^+ is thermodynamically favored (Table I), but at high energies, where both reactions are thermodynamically allowed, MH^+ formation dominates due to angular momentum constraints discussed previously.[8,24]

In the reactions of ammonia with Sc^+, Ti^+, and V^+,[7,8] the sums of the MD^+ and MND_2^+ cross sectioins are smooth functions and the maxima in $\sigma(MD^+)$ are factors of 3–5 larger than the maxima in $\sigma(MND_2^+)$. In the present systems, the total cross sections are not smooth and $\sigma(MD^+)$ are factors of 7–10 larger than $\sigma(MND_2^+)$ at their respective maxima. This behavior suggests that these late transition metal ions also form MH^+ (MD^+) and possibly MNH_2^+ (MND_2^+) via direct reactions without production of intermediate I.

Figure 5 shows the potential energy surfaces for the interaction of Co^+ that can be drawn from these ideas. Results for Ni^+ and Cu^+ should be similar. The initial interaction between Co^+ and ammonia is attractive due to the ion–dipole potential. The depth of this $Co^+··NH_3$ well is given by the Co^+–NH_3 bond strength determined by Marinelli and Squires, 2.55 eV.[6] Bond additivity estimates, i.e., the assumption that $D°(HM^+–NH_2) \approx D°(M^+–NH_2)$, show that formation of I from reactants should be approximately thermoneutral for the Co^+ system and ~0.6 and ~1.6 eV endothermic for the Ni^+ and Cu^+ systems, respectively. Since a tight transition state is presumably required for the isomerization of I to $Co^+··NH_3$, a barrier between these species is included.

In the reactions of Sc^+, Ti^+, and V^+ with ammonia,[7,8] exothermic formation of $MNH^+ + H_2$ is believed to proceed via

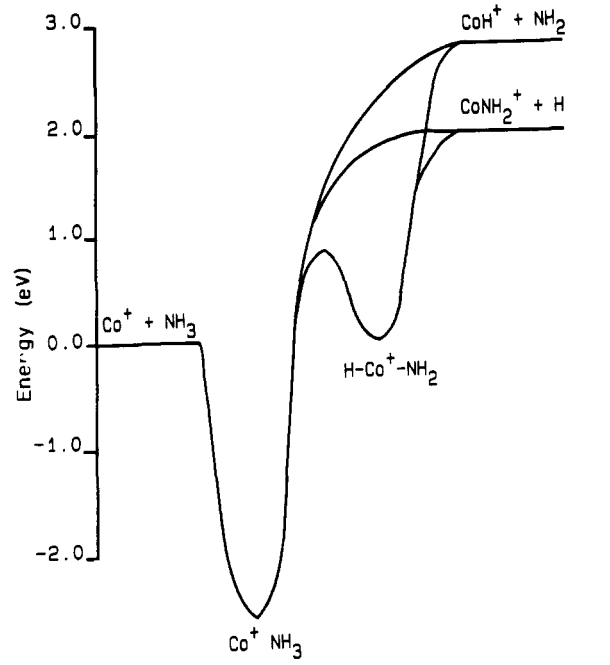

Figure 5. Semiquantitative potential energy diagram for the interaction of Co^+ with NH_3.

dehydrogenation of intermediate I. A definitive explanation for the failure to observe this reaction in the present systems awaits a determination of the energetics of the $CoNH^+$, $NiNH^+$, and $CuNH^+$ species; although Freiser and co-workers have reported that another late transition metal has a weak amide bond energy, $D°(Fe^+–NH) = 2.6 \pm 0.2$ eV.[37] If this is also true for the metals discussed here, then the formation of MNH^+ would be endothermic, although this in itself does not explain why no MNH^+ products are observed. Two plausible explanations can be suggested. A large barrier to the dehydrogenatioin step could exist. Alternatively, the barrier to formation of I, as shown in Figure 5 for Co^+, could prevent formation of this precursor to dehydrogenation until elevated energies. At these higher energies, dehydrogenation (which must require a tight transition state) might no longer compete effectively with reactions 2 and 3. These reactions should be kinetically favored since they involve only simple bond fissions. Similar barriers should exist in the cases of Ni^+ and Cu^+, since intermediate I is even higher in energy than for Co^+, as discussed above.

Considerable insight into this reaction mechanism comes from the adduct species observed in these reactions. The exothermic, pressure-dependent portion of the adduct cross sections must be due to formation of $M^+··NH_3$, the simple adduct where the lone pair of electrons on the nitrogen atom is donated to the metal cation. The lifetimes of these adducts are limited by the reformation of the reactants, as shown by the agreement between the experimental lifetimes and those calculated by RRKM theory.

Finally, we need to explain the pressure-independent formation of $CoNH_3^+$ and $CoND_3^+$ observed at energies above 1 eV. Our observation of a stable, long-lived species with so few constituent atoms is quite unusual. As discussed previously,[10] we assign this feature to formation of a distinct isomer of $CoNH_3^+$, namely intermediate I, $H–Co^+–NH_2$. This structure can explain the long lifetime of this species since the only low-energy pathway for its loss is re-formation of the Co^+ + ammonia reactants, a reductive elimination process that requires going through the tight transition state shown in Figure 5. The height of this barrier is given by the threshold measured for formation of this feature, ~0.8 eV for $H–Co^+–NH_2$ and ~0.9 eV for $D–Co^+–ND_2$. This small difference is consistent with the 0.12 eV zero-point energy difference in $D°(H_2N–H)$ vs $D°(D_2N–D)$.[23] Additional evidence

(36) Hofmann, H.-J.; Hobza, P.; Cammi, R.; Tomasi, J.; Zahradnik, R. *J. Mol. Struct. (THEOCHEM)* **1989**, *201*, 339–350.

(37) MacMahon, T. J.; Freiser, B. S. Unpublished results as reported in: Buckner, S. W.; Gord, J. R.; Freiser, B. S. *J. Am. Chem. Soc.* **1988**, *110*, 6606–6612.

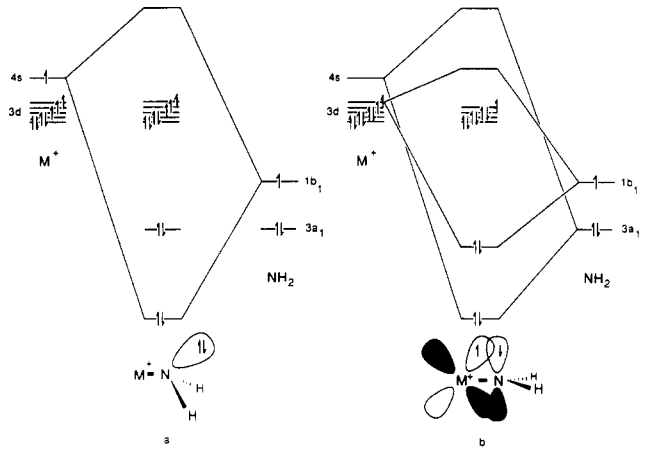

Figure 6. Molecular orbital diagram for interaction of an atomic metal ion with NH_2. Part a shows formation of a covalent σ bond by combining the $NH_2(1b_1)$ and M(4s) orbitals. Part b shows formation of a dative σ bond by combining the $NH_2(3a_1)$ and M(4s) orbitals and a covalent π bond by combining the $NH_2(1b_1)$ and M(3dπ) orbitals. The electron configurations shown are appropriate for $Co^+(4s^13d^7)$ in part a and $Co^+(3d^8)$ in part b.

for this structural assignment is furnished by the energy where these cross-section features begin to decline. As shown in Figure 1, the cross section for this intermediate reaches a maximum at the first appearance of $CoND_2^+$ (and a similar observation is made in the NH_3 system).[10] This is consistent with depletion of the insertion intermediate I once formation of $CoNH_2^+$ begins.

A likely explanation for the failure to detect a cross section feature attributable to $H-M^+-NH_2$ for M = Ni and Cu is the relative stability of these species compared to $H-Co^+-NH_2$. The bond additivity estimates made above for intermediate I suggest that $H-Co^+-NH_2$ is about 0.6 and 1.6 eV more stable than $H-Ni^+-NH_2$ and $H-Cu^+-NH_2$, respectively. Thus, these latter intermediates should have much shorter lifetimes, preventing their direct detection.

Appendix A: Qualitative Bonding Model for MNH_2^+

As discussed by Mavridis et al.[26] for $ScNH_2^+$, there are two possible ways that an amide ligand might bond strongly with an atomic metal ion. Qualitative molecular orbital (MO) diagrams are shown in Figure 6 for these two types of interactions. In both cases, the NH_2 ligand has a MO configuration of $...(1b_2)^2(3a_1)^2(1b_1)^1$. First, we can imagine that NH_2 will bond to first-row transition-metal ions like its CH_3 isoelectronic counterpart,[27] by forming a covalent single bond. For MNH_2^+, this is achieved by combining the $NH_2(1b_1)$ orbital with a metal orbital that is primarily the 4s orbital. Thus, the appropriate electron configuration on the metal is $4s^13d^{n-1}$, where the 3d orbitals remain largely nonbonding. In the absence of additional interactions (see below), the nitrogen atom should remain sp^3 hybridized and thus the MNH_2^+ ion will be nonplanar. Second, the bonding could be dominated by a dative interaction where the NH_2 donates its $3a_1$ lone pair of electrons to an empty 4s orbital on $M^+(3d^n)$. In addition, a covalent π bond can be formed by combination of the $NH_2(1b_1)$ and M(3dπ) orbitals. The four remaining metal 3d orbitals are assumed to be largely nonbonding. Now, the nitrogen atom is sp^2 hybridized and the MNH_2^+ ion is planar.

The resulting MO configurations are similar for the two bonding modes (Figure 6). The primary distinction in the two bonding modes is the extent of the π interaction; however, this distinction is somewhat artificial since, in Figure 6a, the nitrogen lone pair electrons could donate electron density into a metal 3dπ orbital, thus forming a M–N π bond. If this is a strong interaction, then the MNH_2^+ ion could become planar, dissolving the distinctions between parts a and b of Figure 6 and leading to considerable configuration interaction between the two bonding modes. For metals on the left side of the periodic table, this π-bonding interaction should be fairly strong since the antibonding π^* orbital need not be occupied. Indeed, the calculations of Mavridis et al.[26] on $ScNH_2^+$ show that the ground state is planar, although the energy required for bending is quite small (<1 kcal/mol for moving Sc^+ 20° out of the plane). For metals on the right side of the periodic table, the 3d metal orbitals are more than half-filled such that there are two choices. If the MNH_2^+ species is high spin, then the π^* MO must be at least singly occupied for both bonding modes, as illustrated for $CoNH_2^+$ in Figure 6a. This will suppress the π-bonding interaction, which should make the MNH_2^+ ion distort from planarity. Alternatively, the molecule could choose a low-spin configuration in which the π^* orbital is unoccupied, as illustrated for $CoNH_2^+$ in Figure 6b.

$ScNH_2^+$ is calculated to have an MO configuration of $\sigma^2\pi^23d^1$ leading to a $^2A_2$ state (for occupation of the $3d\delta(a_2)$ orbital).[26] As electrons are added they will go into the largely nonbonding 3dδ and second 3dπ orbitals, leading to $TiNH_2^+(\sigma^2\pi^23d^2)$ and $VNH_2^+(\sigma^2\pi^23d^3)$. $CrNH_2^+$ must add an electron into the 3dσ orbital and this should cause some destabilization of the bonding. It seems likely that $MnNH_2^+$ will want a $\sigma^2\pi^23d^5$ configuration in order to retain the stable half-filled $3d^5$ shell. As discussed in the text, Cu^+ may prefer to retain its stable filled $3d^{10}$ shell, such that only the dative bond is formed. For the intermediate cases of $FeNH_2^+$, $CoNH_2^+$, $NiNH_2^+$, it is hard to predict from these qualitative considerations which bonding mode will dominate and whether these species should have high or low-spin configurations. Theoretical calculations are clearly desirable to answer these questions.

TABLE IV: Vibrational Frequencies (cm^{-1}) Used in RRKM Calculations[a]

MNH_3^+	NH_3	MND_3^+	ND_3
898	950	810	748
1117		866	
1125		895	
1153		946	
1537	1627	1164	1191
1547	1627	1164[b]	1191
3142	3337	2294	2420
3382	3444	2384	2564
3393	3444	2532	2564

[b] This frequency was not observed in ref 3. The choice of this value is discussed in the Appendix.

Appendix B: Details of RRKM Calculations

Equation 9 gives the expression for the unimolecular rate of dissociation from RRKM theory. Here, $E^\ddagger$ is the internal energy of the activated complex

$$k_d(E^*) = N(E^\ddagger)/h\rho(E^*) \quad (9)$$

E^* is the internal energy of the energized molecule, $N(E^\ddagger)$ is the sum of accessible states of the activated complex, and $\rho(E^*)$ is the density of states of the energized molecule. In this system, $E^\ddagger$ is just the translational energy of the reactants and $E^* = E^\ddagger + D°(M^+–\text{ammonia})$.

Table IV lists the vibrational frequencies used in these calculations. We have assumed that the vibrational frequencies of gas-phase M^+–ammonia species can be characterized by the $CuNH_3$ and $CuND_3$ frequencies measured in cryogenic argon matrices.[3] For $CuNH_3$, all nine vibrations were observed. However, for $CuND_3$, only eight frequencies were obtained. The missing value was chosen by comparison with the $CuNH_3$ frequencies. At the energy used in this calculation, $E^\ddagger$ is sufficiently low that only the ground vibrational state of the transition state is populated. These are also given in Table IV. We calculate $\rho(E^*)$ by using the Whitten–Rabinovitch approximation.[38]

Acknowledgment. This work is supported by the National Science Foundation, Grant No. CHE-8917980. D.E.C. also thanks L. S. Sunderlin for helpful comments.

(38) Whitten, G. Z.; Rabinovitch, B. S. *J. Chem. Phys.* **1963**, *38*, 2466.